Biomedical Optics EXPRESS

Fluorescent labeling of *Acanthamoeba* assessed *in situ* from corneal sectioned microscopy

Susana Marcos,[1,*] Jose Requejo-Isidro,[1,2] Jesus Merayo-Lloves,[3,4] A. Ulises Acuña,[5] Valentin Hornillos,[5] Eugenia Carrillo,[6] Pablo Pérez-Merino,[1,3] Susana del Olmo-Aguado,[3,4] Carmen del Aguila,[7] Francisco Amat-Guerri,[8] and Luis Rivas[6]

[1]*Instituto de Óptica "Daza de Valdés", Consejo Superior de Investigaciones Científicas, C/Serrano 121, 28006 Madrid, Spain*
[2]*Unidad de Biofísica, Consejo Superior de Investigaciones Científicas-UPV-EHU, Barrio Sarriena s/n. 48940 Leioa (Bizkaia), Spain*
[3]*Instituto de Oftalmobiología Aplicada,Universidad de Valladolid,, Campus Miguel Delibes. Paseo de Belen 17, 47011 28006 Valladolid, Spain*
[4]*Fundación de Investigación Oftalmológica, Instituto Oftalmológico Fundación Fernández-Vega, Avda. Doctores Fernández-Vega 34, 33012 Oviedo, Spain*
[5]*Instituto de Química-Física Rocasolano, Consejo Superior de Investigaciones Científicas, C/Serrano 119, 28006 Madrid, Spain*
[6]*Centro de Investigaciones Biológicas, Consejo Superior de Investigaciones Científicas, C/Ramiro de Maeztu 9, 28040 Madrid, Spain*
[7]*Facultad de Farmacia, Universidad San Pablo-CEU Urb. Montepríncipe, Ctra. Boadilla del Monte, Km. 5.300, 28668 Madrid, Spain*
[8]*Instituto de Química Orgánica, Consejo Superior de Investigaciones Científicas, C/Juan de la Cierva 3, 28006 Madrid, Spain*
**susana@io.cfmac.csic.es*

Abstract: *Acanthamoeba* keratitis is a serious pathogenic corneal disease, with challenging diagnosis. Standard diagnostic methods include corneal biopsy (involving cell culture) and *in vivo* reflection corneal microscopy (in which the visualization of the pathogen is challenged by the presence of multiple reflectance corneal structures). We present a new imaging method based on fluorescence sectioned microscopy for visualization of *Acanthamoeba*. A fluorescent marker (MT-11-BDP), composed by a fluorescent group (BODIPY) inserted in miltefosine (a therapeutic agent against *Acanthamoeba*), was developed. A custom-developed fluorescent structured illumination sectioned corneal microscope (excitation wavelength: 488 nm; axial/lateral resolution: 2.6 μm/0.4-0.6 μm) was used to image intact enucleated rabbit eyes, injected with a solution of stained *Acanthamoeba* in the stroma. Fluorescent sectioned microscopic images of intact enucleated rabbit eyes revealed stained *Acanthamoeba* trophozoites within the stroma, easily identified by the contrasted fluorescent emission, size and shape. Control experiments show that the fluorescent maker is not internalized by corneal cells, making the developed marker specific to the pathogen. Fluorescent sectioned microscopy shows potential for specific diagnosis of *Acanthamoeba* keratitis. Corneal confocal microscopy, provided with a fluorescent channel, could be largely improved in specificity and sensitivity in combination with specific fluorescent marking.

OCIS codes: (180.0180) Microscopy; (170.4470) Ophthalmology; (170.4460) Ophthalmic optics and devices.

References and links

1. J. D. Auran, M. B. Starr, and F. A. Jakobiec, "*Acanthamoeba* keratitis. A review of the literature," Cornea **6**(1), 2–26 (1987).
2. J. Y. Niederkorn, H. Alizadeh, H. Leher, and J. P. McCulley, "The pathogenesis of *Acanthamoeba* keratitis," Microbes Infect. **1**(6), 437–443 (1999).

#170423 - $15.00 USD Received 11 Jun 2012; rev. 31 Jul 2012; accepted 31 Jul 2012; published 12 Sep 2012

3. Z. A. Polat, S. Ozcelik, A. Vural, E. Yildiz, and A. Cetin, "Clinical and histologic evaluations of experimental *Acanthamoeba* keratitis," Parasitol. Res. **101**(6), 1621–1625 (2007).
4. D. Kovacević, T. Misljenović, N. Misljenović, M. Mikulicić, and D. Dabeska-Novkovski, "*Acanthamoeba* keratitis—importance of the early diagnosis," Coll. Antropol. **32**(Suppl 2), 221–224 (2008).
5. A. S. Bacon, J. K. Dart, L. A. Ficker, M. M. Matheson, and P. Wright, "*Acanthamoeba* keratitis. The value of early diagnosis," Ophthalmology **100**(8), 1238–1243 (1993).
6. G. Pasricha, S. Sharma, P. Garg, and R. K. Aggarwal, "Use of 18S rRNA gene-based PCR assay for diagnosis of *Acanthamoeba* keratitis in non-contact lens wearers in India," J. Clin. Microbiol. **41**(7), 3206–3211 (2003).
7. O. Zamfir, H. Yera, T. Bourcier, L. Batellier, J. Dupouy-Camet, C. Tourte-Schaeffer, and C. Chaumeil, "Diagnostic par PCR des kératites à *Acanthamoeba* spp. [Diagnosis of *Acanthamoeba* spp. keratitis with PCR]," J. Fr. Ophtalmol. **29**(9), 1034–1040 (2006).
8. P. P. Thompson, R. P. Kowalski, R. M. Q. Shanks, and Y. J. Gordon, "Validation of real-time PCR for laboratory diagnosis of *Acanthamoeba* keratitis," J. Clin. Microbiol. **46**(10), 3232–3236 (2008).
9. M. Niyyati, J. Lorenzo-Morales, M. Mohebali, S. Rezaie, F. Rahimi, Z. Babaei, C. M. Martín-Navarro, S. Farnia, B. Valladares, and M. Rezaeian, "Comparison of a PCR-based method with culture and direct examination for diagnosis of *Acanthamoeba* keratitis," Iran. J. Parasitol. **4**, 38–43 (2009).
10. Z. Xuejun, L. Xiaoyan, S. Xiaoji, X. Guoxing, and H. Jianzhang, "Application of 28S rDNA PCR technique in the laboratory diagnosis of *Acanthamoeba* keratitis in the clinical," Guoji Yanke Zazhi **9**, 715–718 (2009).
11. W. D. Mathers, S. E. Nelson, J. L. Lane, M. E. Wilson, R. C. Allen, and R. Folberg, "Confirmation of confocal microscopy diagnosis of *Acanthamoeba* keratitis using polymerase chain reaction analysis," Arch. Ophthalmol. **118**(2), 178–183 (2000).
12. D. R. Pfister, J. D. Cameron, J. H. Krachmer, and E. J. Holland, "Confocal microscopy findings of *Acanthamoeba* keratitis," Am. J. Ophthalmol. **121**(2), 119–128 (1996).
13 K. Winchester, W. D. Mathers, J. E. Sutphin, and T. E. Daley, "Diagnosis of *Acanthamoeba* keratitis *in vivo* with confocal microscopy," Cornea **14**(1), 10–17 (1995).
14. J. D. Auran, M. B. Starr, C. J. Koester, and V. J. LaBombardi, "*In vivo* scanning slit confocal microscopy of *Acanthamoeba* keratitis. A case report," Cornea **13**(2), 183–185 (1994).
15. P. K. Vaddavalli, P. Garg, S. Sharma, V. S. Sangwan, G. N. Rao, and R. Thomas, "Role of confocal microscopy in the diagnosis of fungal and *Acanthamoeba* keratitis," Ophthalmology **118**(1), 29–35 (2011).
16. A. Shiraishi, T. Uno, N. Oka, Y. Hara, M. Yamaguchi, and Y. Ohashi, "*In vivo* and *in vitro* laser confocal microscopy to diagnose *Acanthamoeba* keratitis," Cornea **29**(8), 861–865 (2010).
17. E. Nakano, M. Oliveira, W. Portellinha, D. de Freitas, and K. Nakano, "Confocal microscopy in early diagnosis of *Acanthamoeba* keratitis," J. Refract. Surg. **20**(5 Suppl), S737–S740 (2004).
18. S. Hauber, H. Parkes, R. Siddiqui, and N. A. Khan, "The use of high-resolution ^{1}H nuclear magnetic resonance (NMR) spectroscopy in the clinical diagnosis of *Acanthamoeba*," Parasitol. Res. **109**(6), 1661–1669 (2011).
19. H. Y. Tan, Y. Sun, W. Lo, S. W. Teng, R. J. Wu, S. H. Jee, W. C. Lin, C. H. Hsiao, H. C. Lin, Y. F. Chen, D. H. Ma, S. C. Huang, S. J. Lin, and C. Y. Dong, "Multiphoton fluorescence and second harmonic generation microscopy for imaging infectious keratitis," J. Biomed. Opt. **12**(2), 024013 (2007).
20. N. Morishige, W. M. Petroll, T. Nishida, M. C. Kenney, and J. V. Jester, "Noninvasive corneal stromal collagen imaging using two-photon-generated second-harmonic signals," J. Cataract Refract. Surg. **32**(11), 1784–1791 (2006).
21. J. M. Bueno, E. J. Gualda, A. Giakoumaki, P. Pérez-Merino, S. Marcos, and P. Artal, "Multiphoton microscopy of ex vivo corneas after collagen cross-linking," Invest. Ophthalmol. Vis. Sci. **52**(8), 5325–5331 (2011).
22. G. S. Visvesvara, H. Moura, and F. L. Schuster, "Pathogenic and opportunistic free-living amoebae: *Acanthamoeba* spp., *Balamuthia mandrillaris, Naegleria fowleri,* and *Sappinia diploidea*," FEMS Immunol. Med. Microbiol. **50**(1), 1–26 (2007).
23. T. W. Hahn, T. P. O'Brien, W. J. Sah, and J. H. Kim, "Acridine orange staining for rapid diagnosis of *Acanthamoeba* keratitis," Jpn. J. Ophthalmol. **42**(2), 108–114 (1998).
24. K. R. Wilhelmus, M. S. Osato, R. L. Font, N. M. Robinson, and D. B. Jones, "Rapid diagnosis of *Acanthamoeba* keratitis using calcofluor white," Arch. Ophthalmol. **104**(9), 1309–1312 (1986).
25. H. E. Grossniklaus, G. O. I. V. Waring 4th, C. Akor, A. A. Castellano-Sanchez, and K. Bennett, "Evaluation of hematoxylin and eosin and special stains for the detection of *acanthamoeba* keratitis in penetrating keratoplasties," Am. J. Ophthalmol. **136**(3), 520–526 (2003).
26. J. Walochnik, M. Duchêne, K. A. Seifert, A. Obwaller, T. Hottkowitz, G. Wiedermann, H. Eibl, and H. Aspöck, "Cytotoxic activities of alkylphosphocholines against clinical isolates of *Acanthamoeba* spp," Antimicrob. Agents Chemother. **46**(3), 695–701 (2002).
27. V. Hornillos, E. Carrillo, L. Rivas, F. Amat-Guerri, and A. U. Acuña, "Synthesis of BODIPY-labeled alkylphosphocholines with leishmanicidal activity, as fluorescent analogues of miltefosine," Bioorg. Med. Chem. Lett. **18**(24), 6336–6339 (2008).
28. M. Mrva, M. Garajová, M. Lukáč, and F. Ondriska, "Weak cytotoxic activity of miltefosine against clinical isolates of *Acanthamoeba* spp," J. Parasitol. **97**(3), 538–540 (2011).
29. G. S. Visvesvara and W. Balamuth, "Comparative studies on related free-living and pathogenic amebae with special reference to *Acanthamoeba*," J. Protozool. **22**(2), 245–256 (1975).
30. M. Ren and X. Wu, "Evaluation of three different methods to establish animal models of *Acanthamoeba* keratitis," Yonsei Med. J. **51**(1), 121–127 (2010).
31. M. A. A. Neil, R. Juskaitis, and T. Wilson, "Method of obtaining optical sectioning by using structured light in a conventional microscope," Opt. Lett. **22**(24), 1905–1907 (1997).

#170423 - $15.00 USD Received 11 Jun 2012; rev. 31 Jul 2012; accepted 31 Jul 2012; published 12 Sep 2012

32. J. Requejo-Isidro, "Application of fluorescence sectioned microscopy to the *in-situ* diagnosis *Acanthamoeba* spp. ocular infection," presented at Focus on Microscopy, Krakow, Poland, Apr. 5–8, 2009.
33. S. A. Klotz, C. C. Penn, G. J. Negvesky, and S. I. Butrus, "Fungal and parasitic infections of the eye," Clin. Microbiol. Rev. **13**(4), 662–685 (2000).
34. M. M. Eissa, M. Z. El-Azzouni, E. I. Amer, and N. M. Baddour, "Miltefosine, a promising novel agent for *schistosomiasis mansoni*," Int. J. Parasitol. **41**(2), 235–242 (2011).
35. D. Llull, L. Rivas, and E. García, "*In vitro* bactericidal activity of the antiprotozoal drug miltefosine against *Streptococcus* pneumoniae and other pathogenic streptococci," Antimicrob. Agents Chemother. **51**(5), 1844–1848 (2007).
36. S. L. Croft, K. Seifert, and M. Duchêne, "Antiprotozoal activities of phospholipid analogues," Mol. Biochem. Parasitol. **126**(2), 165–172 (2003).
37. F. J. Pérez-Victoria, M. P. Sánchez-Cañete, K. Seifert, S. L. Croft, S. Sundar, S. Castanys, and F. Gamarro, "Mechanisms of experimental resistance of *Leishmania* to miltefosine: Implications for clinical use," Drug Resist. Updat. **9**(1-2), 26–39 (2006).
38. J. Stave, G. Zinser, G. Grümmer, and R. Guthoff, "Der modifizierte Heidelberg-Retina-Tomograph HRT. Erste Ergebnisse einer *In-vivo*-Darstellung von kornealen Strukturen [Modified Heidelberg retinal tomograph HRT. Initial results of *in vivo* presentation of corneal structures]," Ophthalmologe **99**(4), 276–280 (2002).
39. G. P. Mishra, M. Bagui, V. Tamboli, and A. K. Mitra, "Recent applications of liposomes in ophthalmic drug delivery," J. Drug Deliv. **2011**, 863734 (2011).
40. Z. A. Polat, A. Obwaller, A. Vural, and J. Walochnik, "Efficacy of miltefosine for topical treatment of *Acanthamoeba* keratitis in Syrian hamsters," Parasitol. Res. **110**(2), 515–520 (2012).

1. Introduction

Acanthamoeba keratitis is a rare but serious water-borne parasitic infection of the eye caused by the ubiquitous protozoa *Acanthamoeba*, which can result in permanent visual impairment or blindness. Diagnosing *Acanthamoeba* keratitis is a clinical challenge. Initial symptoms resemble those of bacterial keratitis [1–3], although the clinical management of *Acanthamoeba* keratitis differs substantially. As a result, a rapid and accurate identification of the parasite is crucial to guide the appropriate intervention [4].

The standard diagnosis for *Acanthamoeba* keratitis in suspect patients is made by culture and isolation of organisms from a corneal culture or detection of trophozoites and/or cysts on histopathology [5]. This requires corneal scrapping or collection of a corneal biopsy, and typically takes days to confirm diagnosis. However, a negative culture does not necessarily rule out *Acanthamoeba* infection. Molecular diagnostic assays (based on Polymerase Chain Reaction Analysis) have proved to be more rapid [6–10], as well as more sensitive and specific than smear and culture, but they still require corneal scraping to obtain the samples [11], as well as trained personnel.

In vivo corneal confocal microscopy was proposed in the 90's [11–14] for diagnostic non-invasive imaging of *Acanthamoeba* keratitis, and today it has become a major diagnostic tool of this disease [15–17]. *In vivo* confocal microscopy is based on the acquisition of reflectance images of corneal micro-structures, therefore relying on changes of reflectivity and/or index of refraction of the specimens. The identification of the organisms is therefore purely morphological. However, the multiple reflecting structures in the corneal epithelium and stroma present in the standard confocal microscopy images make this identification challenging, and liable to false positives and negatives. While cysts (10-25 μm in diameter) appear to be more reflective, trophozoites (15-45 μm in diameter) have low reflectance and, in general, are difficult to identify.

While imaging techniques are most promising for the diagnosis of *Acanthamoeba* keratitis, due to their capability of rapid detection and non-invasiveness, efforts are still needed to increase their sensitivity and to relieve the need of image analysis and interpretation from the clinician. These techniques should rely on specific signatures of the pathogen, either endogenous or exogenous.

Non-optical imaging techniques (high resolution 1(H) Nuclear Magnetic Resonance Spectroscopy) have been suggested for clinical diagnosis of *Acanthamoeba* keratitis, analyzing its biomechanical profile, and have proved able to identify *Acanthamoeba* isolates with high specificity and sensitivity [18]. However, it is unlikely that this technique may ever be generalized for *in vivo* diagnosis in a clinical standard ophthalmology setting. Multiphoton fluorescence microscopy has also been suggested as a potential technique for differential

#170423 - $15.00 USD Received 11 Jun 2012; rev. 31 Jul 2012; accepted 31 Jul 2012; published 12 Sep 2012

diagnosis of corneal keratitis [19]. However, and probably because of the lack of endogenous fluorescence specific to the pathogen, preliminary data available in the literature do not show specific differentiation from other corneal structures, although a Second Harmonic Generation mode demonstrated altered collagen distribution in the infected corneal regions. Again, although back-scattered and forward-scattered light multiphoton microscopy of the cornea has been demonstrated *in vitro*, its *in vivo* application is still pending [20,21].

Selective pathogen marking, in combination with confocal microscopy, appears as a realistic route for sensitive and specific *in vivo* imaging diagnosis of *Acanthamoeba* keratitis. The use of fluorescent agents in ocular surface diagnosis is common. In the case of *Acanthamoeba* sp. standard immunofluorescence methods by means of *Acanthamoeba*-specific antisera [22] have been used occasionally to visualize throphozoites and cysts *in vitro*. In addition, acridine orange [23] (a DNA/RNA fluorescent marker) and calcofluor white [24] (a fluorophore with high affinity for polysaccharides), have been shown to label cysts in corneal scrapings and in contact lens solution. Unfortunately, the lack of specificity of these fluorescent markers may be a serious drawback for the intended diagnostic applications. On the other hand, *in vivo* direct visualization of the pathogen in infected corneas by fluorescence optical methods remains, to our knowledge, to be demonstrated [25].

In this study, we present a new suitable fluorescence probe for *Acanthamoeba* and the fluorescence imaging of the marked pathogen in the corneal stroma of a rabbit infection model. The probe is made specific to *Acanthamoeba* keratitis by covalent linking a fluorescent dye to miltefosine, a drug with proven therapeutic potential against *Acanthamoeba* [26]. A home-made sectioned microscope with a fluorescence channel based on structural illumination microscopy was used for imaging the labeled pathogens. The specificity of the probe, the low concentration of fluorescent marker needed for staining, the therapeutic nature of the vehicle, the demonstration of the technique in intact eyes *in vitro*, and the ready availability of *in vivo* corneal confocal microscopes prepared for fluorescence imaging hold promise for a new diagnostic approach of *Acanthamoeba* keratitis.

2. Material and Methods

2.1. Fluorescent marker

The pathogen fluorescencent marker MT-11C-BDP (Fig. 1(b)) was designed by inserting a highly fluorescent and photostable group (BODIPY) within the alkyl chain of miltefosine (MT, hexadecylphosphocoline) (Fig. 1(a)). Details of the synthesis and chemical characterization are described elsewhere [27]. Alkylphosphocholines, such as miltefosine, are quickly internalized by *Acanthamoeba* spp., showing cytoxicity against the pathogen [28]. More specifically, miltefosine has been demonstrated to be useful in the treatment of *Acanthamoeba* keratitis in animal models and has been granted an orphan designation for the treatment of *Acanthamoeba* keratitis in humans by the European Commission:

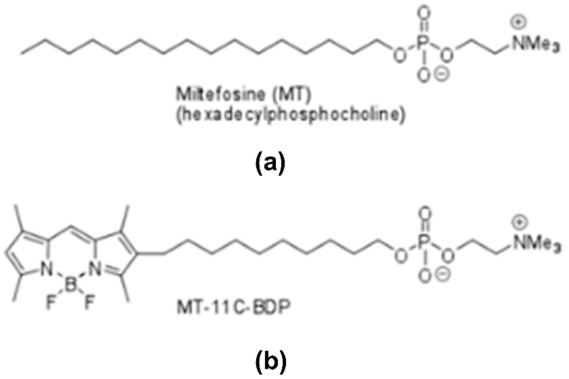

Fig. 1. (a) The alkylphospholipid miltefosine used as carrier of the fluorescent dye. (b) The *Acanthomoeba* fluorescent marker MT-11C-BDP.

#170423 - $15.00 USD Received 11 Jun 2012; rev. 31 Jul 2012; accepted 31 Jul 2012; published 12 Sep 2012

http://www.ema.europa.eu/docs/en_GB/document_library/Orphan_desigantion/2009/10/WC500006373.

The fluorescent marker MT-11C-BDP preserves essential structural motifs of the parent drug, as the phosphocoline head-group and the lipophilic linear alkyl chain. As a result, the antiparasite activity of the marker is identical to that of the original drug [18]. The spectroscopic properties of the marker are those of the emitting BODIPY group, with a fluorescent excitation maximum at 517 nm and the emission peaking at 525 nm.

2. 2. Acanthamoeba culture and staining

Acanthamoeba polyphaga trophozoites (strain 5SU, initially isolated from contact lens from a keratitis patient, and obtained from the collection stocks of Department of Parasitology-Pharmacy School, San Pablo-CEU University Madrid, Spain) were grown at 27°C in PYG + 5% fetal calf serum during 72 hours [29]. Trophozoites were harvested by centrifugation, counted, and resuspended to a concentration of 10^6 cells/ml, following standard protocols. Encystation was obtained by culturing trophozoites in the presence of 50 mM $MgCl_2$ at 30°C [26].

The trophozoites were stained with MT-11C-BDP prior to inoculation in the infection model. The organisms were incubated in 10 μM MT-11C-BDP at 27°C for two hours, followed by successive incubations with free-fatty acid BSA in isotonic saline in order to eliminate non-internalized molecules. The organisms were washed prior to intrastromal injection to ensure that no residual extraamoebic labeled drug remained in the solution prior to injection.

2.3. Corneal infection model

A New Zealand White rabbit was used as a model for *Acanthamoeba* corneal keratitis, by intrastromal injection [30]. The injection was performed into 1/3 of the anterior stroma through a scleral tunnel (3-G needle), parallel to the corneal apex under a surgical microscope. The injected solution (0.1 ml) had a concentration of $2 \cdot 10^5$ cells/ml, with trophozoites incubated with 10 μM BDPY-PC for 1 h. The procedure was conducted *in vivo* with the animal under anesthesia with intramuscular ketamine (37.5 mg/kg; Ketolar, Parke-Davis S.A., Barcelona, Spain) and intramuscular xylazine (5mg/kg; Rompun, Bayer AG, Leverkusen, Germany). In addition, topical anesthesia (0.5% tetracainechlorhydrate and 1 mg oxybuprocaine; Colircusí Anestésico Doble, Alcon Cusí, S.A. Barcelona, Spain) was instilled in the conjunctival fornix. Clinical signs of white corneal stromal infiltrate were present in all animals immediately after injection, and lasted until euthanasia, revealing the presence of the intrastromal *Acanthamoeba* solution.

For control purposes, 10 μL of a solution of 10 μm fluorescent beads (Fluospheres F-8336, Invitrogen) containing 200 beads/μL in PBS was injected into the corneal stroma with identical protocols described above.

A total of 8 rabbits were used in the study. Animals were euthanized with an intravenous injection of 150 mg/kg ketamine hydrochloride, and the enucleated eyes measured less than 6 h post-mortem. The use of animals for this study complies with the ARVO guidelines for animal research. Additional control experiments were performed on virgin enucleated porcine eyes. Eyes were obtained from a local slaughterhouse within 4 h post-mortem.

2.4. Fluorescence corneal sectioning microscopy system

Corneal sectioning microscopy was performed on a home-developed microscope, based on structured illumination, which was specifically adapted for fluorescence imaging. Structured illumination microscopy allows optical sectioning on a wide-field configuration with similar or higher resolution than standard confocal microscopy [31]. Background rejection is based on the fact that high-spatial frequencies, associated with detail in an image, attenuate faster than lower spatial frequencies with defocus. Projection of a high spatial frequency pattern on the focal plane of the sample results in spatial modulation of the in-focus information. Away from the focal plane this high-spatial frequency pattern is quickly attenuated and thus information is

#170423 - $15.00 USD Received 11 Jun 2012; rev. 31 Jul 2012; accepted 31 Jul 2012; published 12 Sep 2012

not modulated out of focus. Demodulation of the 2-D recorded signal allows recovery of the in-focus information.

The system lay-out and properties (for reflectance microscopy) are described in detail elsewhere [32]. In brief, a diffraction grating (20DG50, Comar Optics, UK) located on a plane conjugate to the focal plane was projected through the objective, producing a 2.25 μm sine pattern superimposed to sample image. High-diffracted orders were blocked at the back focal plane of the objective. Phase-images required for retrieval of the in-focus information were obtained shifting the grating with a piezostage (M-663.465 PI, Germany). Images were recorded on a scientific-grade CCD camera (Orca-AG, Hamamatsu Photonics, Japan). Imaging was performed at 488 nm using either a x50, NA0.50 (Olympus LMPLFLN 50X, NA0.50, w.d. 10.6 mm) dry objective or a x40, NA 0.80 water-immersion long working distance objective (Olympus LUMPLFLN 40XW, NA 0.80, w.d. 3.3 mm). Typical total exposure time per sectioned image was less than 30 ms. Data transfer and saving reduced the overall imaging rate to 3.3 Hz at maximal field of view. Fluorescent beads and an ultrathin fluorescent layer dried on a coverslip allowed to determine experimentally the Point Spread Function, revealing a lateral resolution of 0.4 to 0.6 μm (depending on the NA of the objective) and an axial resolution of 2.6 μm FWHM. Typically, a circular area of 60 μm diameter in the sample was measured, with an axial range larger than 500 μm, which allowed imaging from the epithelium to beyond the endothelium into the anterior chamber both in the rabbit cornea and the porcine corneas.

A fluorescence channel was also implemented. The excitation light was provided by a CW 488 nm diode pumped solid state laser (85-BCD, CVI Melles-Griot). A dichroic filter (D535/40, with a bandwidth of 515-555 nm, Chroma Technology Corporation, Bellows Falls, VT, USA) was placed in the detection channel.

2.5. Experimental protocols

Enucleated eyes were placed in custom-designed methacrylate eye-holders mounted on a micro-positioning stage in front of the microscope (with the optical axis parallel to the optical table). For the purposes of this study the immersion objective (x40) was used. An ophthalmic solution (Viscotears, Novartis, refractive index = 1.338 at 488 nm at 25 degrees) allowed optically coupling the cornea to the objective. No applanating optics was used. Images were typically centered around the corneal apex (although other lateral locations were also tested) using a micro-positioning stage (LTA-HS, Newport Co, USA). In-depth scanning was performed at Nyquist resolution, from which three-dimensional images of the sample may be reconstructed. A 3-D stack was typically run at 3 to 9 μm/s .

Rabbits were sacrificed 1 hour after injection of the pathogens. The eyes were immediately enucleated and kept in DMEM/F12 (Invitrogen Corp., Carlsbad, CA, USA) at 4 degrees. All measurements were carried out within 6 h post-mortem.

2.6. Control experiments

Control experiments were performed to evaluate: (1) the fluorescence sectioned imaging capabilities of the microscope within the corneal stroma, (2) the bioactivity and selectivity of the fluorescent probe for *Acanthamoeba* spp.; and (3) the specificity of the compound for *Acanthamoeba* spp., and lack of internalization by healthy corneal cells.

Fluorescence sectioned microscopy images were obtained on rabbit eyes with corneas injected with fluorescence beads, using similar protocols than those followed on corneas infected with *Acanthamoeba* spp.

Also, the bioactivity and selectivity of MT-11C-BDP was established upon inspection of both conventional epifluorescence and optically sectioned fluorescent images of MT-11C-BDP cultured samples of isolated *Acanthamoeba* acquired using the instrument described above. Samples were incubated in a 5 μM solution of MT-11C-BDP for 30 min at room temperature and then imaged on a microscope slide.

The specificity of the labeling of the pathogen by the fluorescent marker MT-11C-BDP was established with the help of a control BODIPY dye (PM567), with a similar structure,

#170423 - $15.00 USD Received 11 Jun 2012; rev. 31 Jul 2012; accepted 31 Jul 2012; published 12 Sep 2012

excitation and emission spectrum and quantum efficiency to those of MT-11C-BPD, but lacking the phosphatidylcholine group head and the alkyl chain. In addition, solutions at the same concentration (5 μM) of both MT-11C-BDP and PM567 were topically applied to uninfected enucleated porcine eyes and left for incubation for times (90 min) much longer than expected in clinical use. Eyes were washed with PBS-BSA prior to imaging. Optically sectioned images in eyes with intact corneas and after mechanical removal of the epithelium (to guarantee the diffusion of the fluorescent compound inside the stroma) were acquired in a non-contact configuration.

3. Results

3.1. Evaluation of the corneal infection model

Figure 2 shows an example of the clinical appearance of the intrastromal infiltrate in rabbit, prior to enucleation. The clinical appearance was similar in both the experimental and control groups, with clear signs of stromal edema.

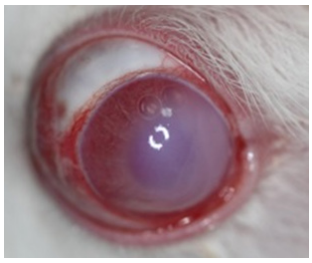

Fig. 2. Example of clinical appearance of a rabbit eye (*in vivo*), following intrastromal injection.

3.2. Control experiments

Images of the fluorescent beads implanted in the corneal stroma of rabbits were successfully achieved in healthy eyes. Figure 3(a) shows a sectioned image (60 μm diameter) of the stroma containing a fluorescent bead.

MT-11C-BDP was efficiently internalized by *Acanthamoeba* trophozoites, whereas for cysts a weak fluorescent rim was observed. Figure 3(b) shows fluorescence sectioned microscopic images of a sample of isolated stained organisms (both trophozoits and cysts). Their morphology and size matches findings from histopathology.

MT-11C-BDP was not internalized by healthy corneal cells. Figure 3(c) and 3(d) show the side (yz plane) and front (xy plane) views of the corneas of uninfected enucleated porcine eyes topically treated with PM567 and MT-11C-BDP, respectively. The vertical white line across the side view indicates the axial (z) location of the front (xy) sectioned image, while the blue arrow on the front image indicates the x location of the lateral view (yz). The left area of the side views (lateral panel of each figure) is the empty space between the objective and the cornea, while the right area corresponds to areas within the cornea. Note also that pixels have been resized so that the scale is the same in all three dimensions. Figure 3(c) shows that the fluorescent emission of PM567 treated eyes is easily detected inside the epithelial cells, while their nuclei remain dark. On the other hand, the fluorescent emission of MT-11C-BDP treated eyes (Fig. 3(d) originates in a layer (side view) of thickness below resolution (<2.6 μm), consistent with the plasma membrane of the epithelial outmost cells. No traces of fluorescent emission inside the epithelial cells could be detected, confirming that MT-11C-BDP is not internalized by healthy epithelial cells. Images of de-epithelized corneas treated with MT-11C-BDP did not reveal staining of other corneal structures (stromal collagen). Figure 3(e) shows images of de-epithelized corneas treated with MT-11C-BDP which did not reveal staining of other corneal structures.

#170423 - $15.00 USD Received 11 Jun 2012; rev. 31 Jul 2012; accepted 31 Jul 2012; published 12 Sep 2012

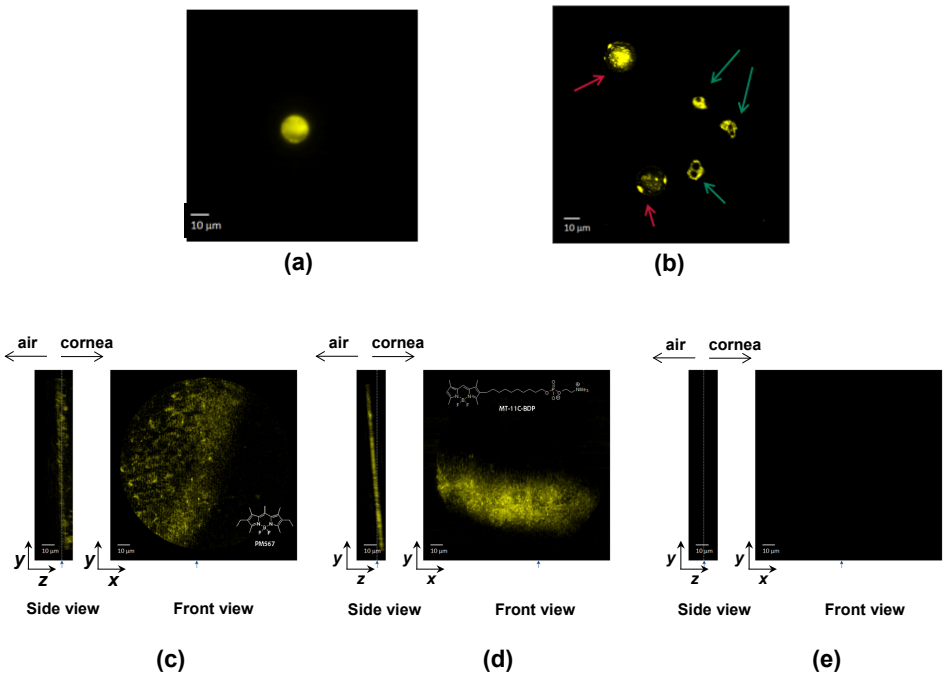

Fig. 3. (a) Fluorescence sectioned image of a fluorescent bead (10 µm) implanted in the corneal stroma of a White New Zealand rabbit. (b) Fluorescence sectioned images of isolated MT-C11-BDP stained *Acanthamoeba* trophozoits (green arrows) and cysts (red arrows). (c) Fluorescent sectioned image of a porcine cornea after topical application of a solution of the BODIPY fluorescent group (PM567, inset) lacking the polar head and the lipidic chain of miltefosine. (d) Fluorescent sectioned image of a porcine cornea after topical application of the fluorescent marker MT-C11-BDP (miltefosine with a BODIPY group, inset). (e) Fluorescent sectioned image of a de-epithelized porcine cornea after topical application of the fluorescent marker MT-C11-BDP (miltefosine with a BODIPY group, inset). Figure 3(c), Fig. 3(d) and Fig. 3(e) show en face images (xy plane, front view) of the cornea at the plane indicated by the dotted line on the lateral plane (yz plane, side view). Epithelial cells in the eye treated with PM567 (Fig. 3(c)) are clearly identified, as fluorescence originates in the cytoplasm while the nuclei remain dark, indicative of the free BODIPY group being internalized by the cells. In contrast, all fluorescent emission in the eye treated with MT-11C-BDP (Fig. 3(d)) originates from a thin layer at the cornea (plasma membrane of epithelial cells), and no other cellular structure is recognized, indicative that when the BODIPY group is bound to miltefosine it is not internalized by healthy epithelial cells or other corneal structures. De-epithelized corneas did not show any detectable fluorescence signal (Fig. 3(e)) upon treatment with MT-11C-BDP in the same conditions as intact corneas (Fig. 3(c) and (d)). No applanating optics or contact medium was used (x50 dry objective, see text) for imaging the corneas in Fig. 3(a), Fig. 3(c), Fig. 3(d) and Fig. 3(e). Isolated trophozoites and cysts in Fig. 3(b) were imaged through a x40, NA1.25 oil objective.

3.3. Fluorescence imaging of amoebas in situ

Acanthamoebae implanted in the stroma were successfully imaged by fluorescence sectioned microscopy. Figure 4 shows a sectioned images (20 µm depth and 50 µm diameter) of the stroma in an infected rabbit eye, where three stained *Acanthamoeba* trophozoites located at the same depth inside the cornea are easily identifiable by their contrasted fluorescent emission, with unstained nucleus or vacuole, and their morphological features, such as size and shape. The left panel shows axial sections, with the dotted line and arrow indicating the axial position of the lateral cross-section shown in the right panel. The right panel shows en face views of the *Acanthamoebae*, with the arrow indicating the lateral location of the corresponding axial section shown in the left panel.

#170423 - $15.00 USD Received 11 Jun 2012; rev. 31 Jul 2012; accepted 31 Jul 2012; published 12 Sep 2012

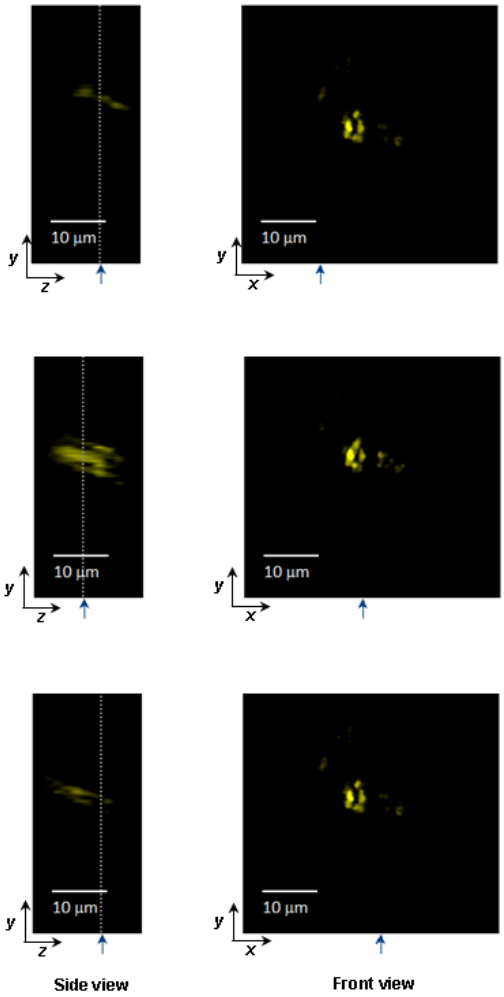

Fig. 4. Fluorescence sectioned image of several MT-C11-BDP- stained *Acanthomoeba* trophozoites, implanted in the stroma of a rabbit eye. Images were obtained in intact enucleated eyes. The left panels show axial images (yz plane, side views). The right panels show en face images (xy plane, front view) of the cornea at the plane indicated by the dotted line on the axial image. The pathogens are easily identified by their morphological features, such as size and shape. A comfort ophthalmic solution was used as immersion medium, but no applanating optics was used for imaging (x40W objective, see text).

4. Discussion

We have presented a fluorescent marker for specific staining of *Acanthamoeba* (cysts and trophozoites), and its potential for *in situ* visualization using fluorescence sectioned microscopy. Although the concept has been evaluated *in vitro*, imaging has been conducted on enucleated intact eyes, under similar conditions of an *in vivo* testing.

The method is, to our knowledge, the first attempt for *in situ* fluorescent-marker based visualization of *Acanthamoeba* in an infected eye. The specificity and sensitivity of the technique exceeds largely that of reflectance corneal confocal microscopy, as the morphological identification of the pathogen is not confounded by other reflective corneal structures. We have demonstrated that other corneal cells or the intrastromal matrix do not internalize the fluorescent compound, making it specific to the pathogen. We have not studied the potential for other ocular pathogenic micro-organisms [33] to incorporate miltefosine, but

#170423 - $15.00 USD Received 11 Jun 2012; rev. 31 Jul 2012; accepted 31 Jul 2012; published 12 Sep 2012

the associated ocular infections by other organisms which could potentially marked by miltefosine (i.e. *Helminths* [34], *Trypanosomatids* or *Leishmania* [35–37]) are rare, and the pathogens could be easily differentiated by their size and their intracellular pattern.

The mechanism by which other fluorescent markers (such as PM567 in our control experiments) are able to enter the cells, while MT-11C-BDP does not, remains to be investigated in full. We hypothesize that PM567 is internalized by a diffusion mechanism, while MT-11C-BDP requires a specific molecular transporter to do so.

The fluorescent marker can also be applied to visualization of *Acanthamoeba* in corneal scrapings or contact lens solutions, but the great potential of the technique relies on its promise for *in vivo* application, which would provide an immediate diagnosis of the suspect patient. An additional advantage of the compound is the use of miltefosine, a demonstrated therapeutic agent against *Acanthamoeba*, although it is not lethal at the very low doses used for diagnosis. Regarding a possible topical corneal application for diagnostics, our experiments show that fluorescent staining of the parasite is much more intense than that of the surrounding tissues, likely due to the presence of an active intracellular pumping mechanism of the drug by these organisms. For *in vitro* diagnosis (corneal scrapings, clinical isolates) the use of a standard quencher of the residual background fluorescence or autofluorescence (Trypan Blue, 0.4%) allows elimination of the fluorescence background.

Although we have used a custom-developed sectioning microscope in this study, the technique could be used with only slight modifications of commercial *in vivo* corneal confocal microscopy, upon the incorporation of a fluorescent channel. Interestingly, a commercial instrument [38] (i.e. Heidelberg Retina Tomograph with the Rostock Cornea Module, Heidelberg Engineering) is equipped with excitation lasers for retinal fluorescein angiography. The wavelength of the laser source (or alternative the excitation peak of the fluorescent marker) could be modified for proper excitation. The requirement for optical sectioning should be emphasized. In conventional wide field fluorescent microscopy, the fluorescent emission of the residual drug accumulating on the outside membrane of healthy epithelial cells may hinder the emission from the pathogens. Also, the infiltrates can be multifocal and, in a clinical setting, the amoebae are not necessarily most numerous in the area of the most obvious infiltrate. The use of a scanning sectioning technique, however, has become common practice in the evaluation of *Acanthomoeba* keratitis subjects. Besides the topical application of the fluorescent compound and use of the fluorescent mode of the instrument, corneal examination for *Acanthomoeba* keratitis with the proposed method could follow similar protocols than those currently performed with the reflectance corneal confocal microscope.

In this study, the pathogens were stained before injection in the corneal stroma. Interestingly, the lifetime of the probe was at least 6 h, a timeline much longer than that of a typical clinical examination. However, the diffusion of the compound in the stroma of an infected eye and the subsequent staining of the pathogens in situ remains to be tested. Clinical application of the method could involve de-epithelization of the patient's cornea to facilitate the diffusion of the compound for fluorescent imaging. Alternatively, the use of drug delivery formulations capable of transporting the compound through the corneal epithelium barrier can be explored [39]. Toxicology tests are also pending. However, the low concentrations of the fluorescent compound (more than three orders of magnitude lower than standard fluorescein routinely used topically on the cornea) and the lack of chemical reactivity of the emitting group anticipate low toxicity potential. On the other hand, miltefosine is an approved compound for topical application in the eye for therapeutical treatment of *Acanthamoeba* keratitis, with a concentration ~16 times higher than that used in the current study for diagnostic purposes [40].

Finally, *in vivo* application of the technique would require slightly lower corneal incident power than that used in the current *in vitro* study, in order to remain within the standards of maximum permitted exposure (0.065 μJ for a SIM microscope or 0.045 μJ for a confocal microscope for an imaged area of 0.01 mm^2 at the illumination wavelength used in this work (American National Standards Institute (ANSI)). Different hardware configurations of the

#170423 - $15.00 USD Received 11 Jun 2012; rev. 31 Jul 2012; accepted 31 Jul 2012; published 12 Sep 2012

instrument would make the system more light-efficient, such as a different imaging strategy (confocal, line scanning, etc.), longer excitation wavelength or more sensitive detectors, among others. On the other hand, the study has been performed under very conservative compound concentrations, and it is likely that doses may increase after a drug-toxicity study.

5. Conclusions

We have shown a fluorescent-based sectioned microscopy imaging technique for visualization of *Acanthamoeba* keratitis, with highly specific labeling for the pathogens (and no other internal corneal structures) in a rabbit model. The selective marker is based on a bright, photo-stable, fluorescent compound (a BODIPY chromophore) inserted into the lipid tail of miltefosine, an approved therapeutic drug for *Acanthamoeba*, which provides it with high specificity. Optical sectioning allows acquisition of high contrast images that would otherwise be masked by a strong fluorescent background from the membrane of epithelial cells. *In vivo* confocal corneal microscopes, available clinically, could be modified to add the fluorescence channel required for fluorescence detection. The technique holds promise for *in vivo* diagnosis of *Acanthamoeba* keratitis.

Acknowledgments

The authors acknowledge funding from a CSIC Proyecto Intramural Frontera PIF80F0171/2/3; Ministerio de Ciencia e Innovación, Spain, FIS2008-02065 (S. M.), FIS2011-25637 (S. M.), RYC2006-2920 (J. R. I.), FIS2009-07966 (J. R. I.), CTQ2010-16457 (A. U. A.), PROFIT CIT-300100-2007-50 (J. M. L.); Instituto de Salud Carlos III ISCIII-(RICET)-FEDER RD 06/0021/0006 (L. R.), and FIS 2009-01928 (L. R.); European Union FP7 HEALTH-2007-223414 (L. R.); EURHORCS-ESF Grant EURYI-05-102-ES (S. M.). The authors also acknowledge the Unidad Asociada IOBA-UVA/IO-CSIC. The authors (S. M., A. U. A., V. H., J. M. L., J. R. I., E. C., F. A., C. dA., L. R.) disclose their participation as inventors in a related patent ("F. luorescent miltefosine analogs for diagnosis of infectious diseases," Spanish patent application P200800951, PCT/ES2011/070077).